SIMBAD Pipeline entry

A&A Meeting
06/03/2020

CENTRE DE DONNÉES ASTRONOMIQUES DE STRASBOURG

OBERTO A.
MANTELET G.

Current process
A&A → SIMBAD

- Table Of Content:

  → *(FTP XML, python script)* bibliography in SIMBAD

- Text:

  → *(EDP PDF, DJIN)* object name & small tables data in SIMBAD

- Tables (big):

  → *(VizieR, COSIM)* table data in SIMBAD

New process

- Table Of Content + Article text

  → *(FTP XML, bash script)* ***XCDS***

    → *(XCDS)* bibliography in SIMBAD

    → *(XCDS, DJIN)* object name & small tables in SIMBAD

- Tables (big):

    → *(XCDS/VizieR, COSIM)* table data in SIMBAD

1 - Download

- Once a volume id finished : download from FTP cdsarc all gz files
- Extract all files from one volume (some articles are replaced)
  - XML, JPEG, PDF ...

□ 2 - Convert

- XSLT Filters to transform XML
  - → XCDS for DJIN
    - → TOC for SIMBAD
- + extra characters / formula

3 – Name recognition

- DJIN parsing to extract object names

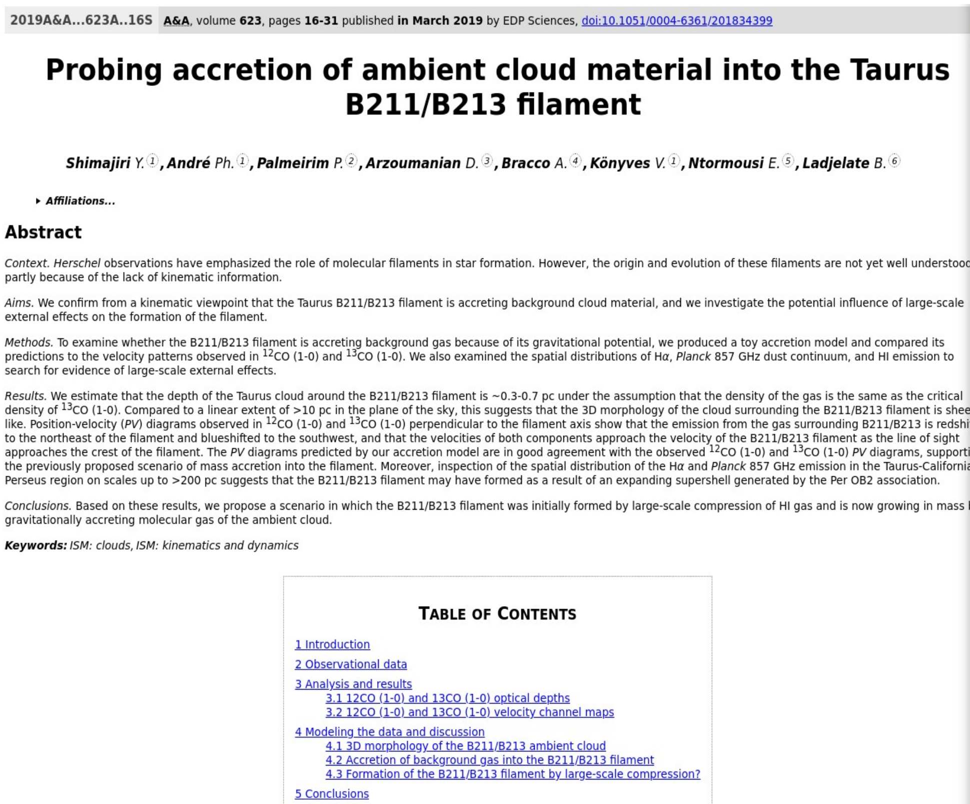
2019A&A...623A..16S **A&A**, volume **623**, pages **16-31** published **in March 2019** by EDP Sciences, doi:10.1051/0004-6361/201834399

Probing accretion of ambient cloud material into the Taurus B211/B213 filament

***Shimajiri** Y.* [1], ***André** Ph.* [1], ***Palmeirim** P.* [2], ***Arzoumanian** D.* [3], ***Bracco** A.* [4], ***Könyves** V.* [1], ***Ntormousi** E.* [5], ***Ladjelate** B.* [6]

▸ *Affiliations...*

Abstract

Context. *Herschel* observations have emphasized the role of molecular filaments in star formation. However, the origin and evolution of these filaments are not yet well understood, partly because of the lack of kinematic information.

Aims. We confirm from a kinematic viewpoint that the Taurus B211/B213 filament is accreting background cloud material, and we investigate the potential influence of large-scale external effects on the formation of the filament.

Methods. To examine whether the B211/B213 filament is accreting background gas because of its gravitational potential, we produced a toy accretion model and compared its predictions to the velocity patterns observed in ^{12}CO (1-0) and ^{13}CO (1-0). We also examined the spatial distributions of Hα, *Planck* 857 GHz dust continuum, and HI emission to search for evidence of large-scale external effects.

Results. We estimate that the depth of the Taurus cloud around the B211/B213 filament is ~0.3-0.7 pc under the assumption that the density of the gas is the same as the critical density of ^{13}CO (1-0). Compared to a linear extent of >10 pc in the plane of the sky, this suggests that the 3D morphology of the cloud surrounding the B211/B213 filament is sheet like. Position-velocity (*PV*) diagrams observed in ^{12}CO (1-0) and ^{13}CO (1-0) perpendicular to the filament axis show that the emission from the gas surrounding B211/B213 is redshif to the northeast of the filament and blueshifted to the southwest, and that the velocities of both components approach the velocity of the B211/B213 filament as the line of sight approaches the crest of the filament. The *PV* diagrams predicted by our accretion model are in good agreement with the observed ^{12}CO (1-0) and ^{13}CO (1-0) *PV* diagrams, supportir the previously proposed scenario of mass accretion into the filament. Moreover, inspection of the spatial distribution of the Hα and *Planck* 857 GHz emission in the Taurus-California Perseus region on scales up to >200 pc suggests that the B211/B213 filament may have formed as a result of an expanding supershell generated by the Per OB2 association.

Conclusions. Based on these results, we propose a scenario in which the B211/B213 filament was initially formed by large-scale compression of HI gas and is now growing in mass b gravitationally accreting molecular gas of the ambient cloud.

Keywords: *ISM: clouds, ISM: kinematics and dynamics*

TABLE OF CONTENTS

1 Introduction
2 Observational data
3 Analysis and results
3.1 12CO (1-0) and 13CO (1-0) optical depths
3.2 12CO (1-0) and 13CO (1-0) velocity channel maps
4 Modeling the data and discussion
4.1 3D morphology of the B211/B213 ambient cloud
4.2 Accretion of background gas into the B211/B213 filament
4.3 Formation of the B211/B213 filament by large-scale compression?
5 Conclusions
Acknowledgements

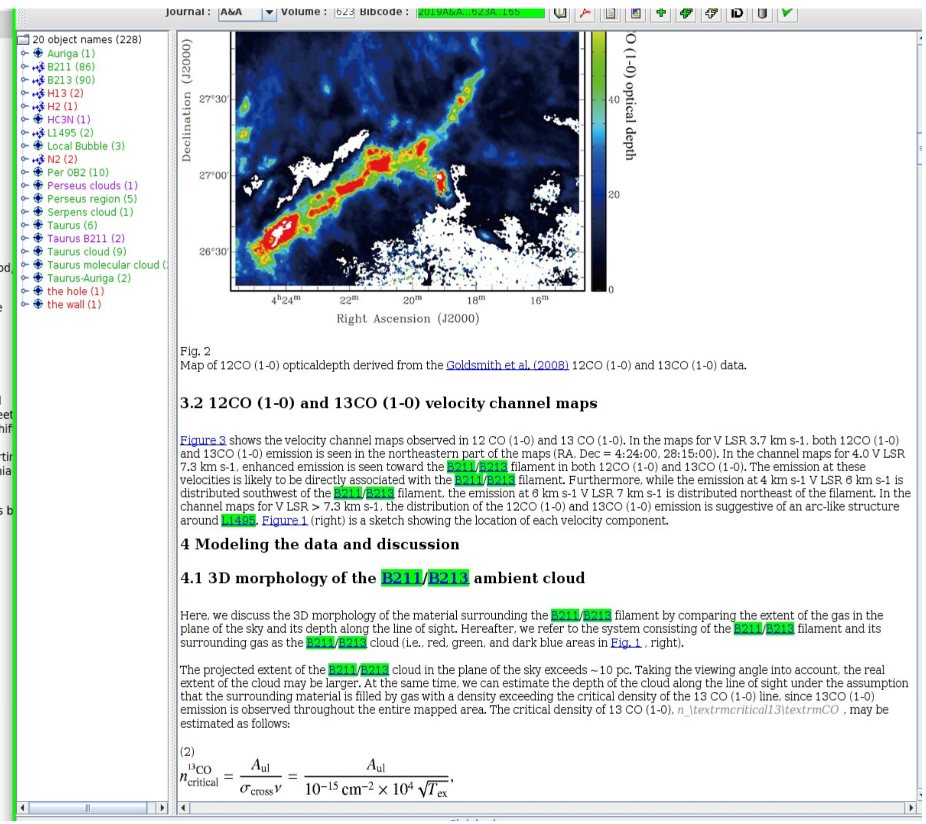

Fig. 2
Map of 12CO (1-0) opticaldepth derived from the Goldsmith et al. (2008) 12CO (1-0) and 13CO (1-0) data.

3.2 12CO (1-0) and 13CO (1-0) velocity channel maps

Figure 3 shows the velocity channel maps observed in 12 CO (1-0) and 13 CO (1-0). In the maps for V LSR 3.7 km s-1, both 12CO (1-0) and 13CO (1-0) emission is seen in the northeastern part of the maps (RA, Dec = 4:24:00, 28:15:00). In the channel maps for 4.0 V LSR 7.3 km s-1, enhanced emission is seen toward the B211/B213 filament in both 12CO (1-0) and 13CO (1-0). The emission at these velocities is likely to be directly associated with the B211/B213 filament. Furthermore, while the emission at 4 km s-1 V LSR 6 km s-1 is distributed southwest of the B211/B213 filament, the emission at 6 km s-1 V LSR 7 km s-1 is distributed northeast of the filament. In the channel maps for V LSR > 7.3 km s-1, the distribution of the 12CO (1-0) and 13CO (1-0) emission is suggestive of an arc-like structure around L1495. Figure 1 (right) is a sketch showing the location of each velocity component.

4 Modeling the data and discussion

4.1 3D morphology of the B211/B213 ambient cloud

Here, we discuss the 3D morphology of the material surrounding the B211/B213 filament by comparing the extent of the gas in the plane of the sky and its depth along the line of sight. Hereafter, we refer to the system consisting of the B211/B213 filament and its surrounding gas as the B211/B213 cloud (i.e., red, green, and dark blue areas in Fig. 1 , right).

The projected extent of the B211/B213 cloud in the plane of the sky exceeds ~10 pc. Taking the viewing angle into account, the real extent of the cloud may be larger. At the same time, we can estimate the depth of the cloud along the line of sight under the assumption that the surrounding material is filled by gas with a density exceeding the critical density of the 13 CO (1-0) line, since 13CO (1-0) emission is observed throughout the entire mapped area. The critical density of 13 CO (1-0), n_\textrmcritical13\textrmCO , may be estimated as follows:

(2)

$$n^{^{13}\mathrm{CO}}_{\mathrm{critical}} = \frac{A_{\mathrm{ul}}}{\sigma_{\mathrm{cross}}\,v} = \frac{A_{\mathrm{ul}}}{10^{-15}\,\mathrm{cm}^{-2}\times 10^{4}\sqrt{T_{\mathrm{ex}}}},$$

4 – Table data

- COSIM extract columns from tables (VizieR)
  - Xmatch with SIMBAD to add some data